Research Article

Slip flow of Jeffrey nanofluid with activation energy and entropy generation applications

Hu Ge-JiLe[1], Sumaira Qayyum[2], Faisal Shah[2] (iD), M Ijaz Khan[3] (iD) and Sami Ullah Khan[4]

Abstract
The growing development in the thermal engineering and nano-technology, much attention has been paid on the thermal properties of nanoparticles which convey many applications in industrial, technological and medical era of sciences. The noteworthy applications of nano-materials included heat transfer enhancement, thermal energy, solar systems, cooling of electronics, controlling the heat mechanisms etc. Beside this, entropy generation is an optimized scheme which reflects significances in thermodynamics systems to control the higher energy efficiency. On this end, present work presents the slip flow of Jeffrey nanofluid over a stretching sheet with applications of activation energy and viscous dissipation. The entropy generation features along with Bejan number significance is also addressed in present analysis. Buongiorno model of nanofluid is used to discuss the heat and mass transfer. The formulated flow equations are attained into non-dimensional form. An appropriate ND MATHEMATICA built-in scheme is used to find the solution. The solution confirmation is verified by performing the error analysis. For developed flow model and impacted parameters, a comprehensive graphical analysis is performed. It is observed that slip phenomenon is used to decays the velocity profile. Temperature and concentration are in direct relation with Brownian motion parameter and activation energy respectively. Entropy and Bejan number have same results for greater diffusion parameter.

Keywords
Jeffrey fluid, slip condition, entropy generation, bejan number, nanofluid, activation energy, viscous dissipation

Date received: 6 February 2021; accepted: 5 March 2021

Handling Editor: James Baldwin

Introduction

The non-Newtonian fluids attribute the importance in era of industries and technologies and scientists have paid special attention by exploring distinct rheological mechanism. Different researches have been conducted on the dynamics of gases and he proposed a theory to explain different properties of gases. Scientists also work on the pseudo-plastic liquids and constituted expressions for them. Scientists have also worked on the properties and behavior of Bingham like viscous materials which referred to the significances of lubrication flows. Ramesh[1] worked on two types of flow Couette and Poiseuille flows of Jeffrey fluid. Jeffrey

fluid flow through porous medium and Soret and Dufour effect has been worked out by Kumar and

[1]School of Science, Huzhou University, Huzhou, Zhejiang, P. R. China
[2]Department of Mathematics, Quaid-I-Azam University, Islamabad, Pakistan
[3]Department of Mathematics and Statistics, Riphah International University, Islamabad, Pakistan
[4]Department of Mathematics, COMSATS University Islamabad, Sahiwal, Pakistan

Corresponding author:
Faisal Shah, Department of Mathematics, Quaid-I-Azam University, Islamabad 44000, Pakistan.
Email: sfaisal@math.qau.edu.pk

co-researchers.[2] Ramesh et al.[3] discussed the motion of Casson fluid with stagnation point over variable thickness. Xun et al.[4] discussed the rheological behavior of Ostwald-de Waele fluid confined by rotating disk. Farooq et al.[5] elucidated the radiative flow of viscoelastic nanofluid. Some more recent analysis expressing the rheological mechanism of non-Newtonian materials can be shown in Refs.[6–10]

The nano-materials are the materials that contain particles in the size range of 1–100 nm. A lot of research has been done on the properties and studies of nano materials in the last few years because of their wide range of applications in many fields. They have many applications in different fields like in engineering, nano technology micro manufacturing and in pharmaceutical processes as well. There main applications of such materials in industries, technologies and thermal sciences. The utilization of nanoparticles significantly improves the efficiency of heat transfer processes. The heat transfer increases due to suspension of nano particles in the base fluid. The stability of nano materials is very important so that the thermo physical characteristics of the material are maintained after fabrication process. Many researches have been conducted on it and still researchers are working on it due to their applications in various fields. Choi and Eastman[11] was one who first discovered the nanofluid flow. Hayat et al.[12] examined the entropy generation in Ag and Cu water nanofluid. Krishnamurthy et al.[13] analyzed the convective thermal transport of nanoparticles in presence of slip effects and porous space. Kumar et al.[14] inspected the Marangoni flow of Casson nanofluid with dynamic impact of chemical reaction and heat generation mechanism. The features of entropy generation, viscous dissipation in radiative flow of micropolar nanofluid have been suggested by Roja et al.[15] Hamid et al.[16] addressed the heat transfer enhancement in water-based carbon nanotubes configured by heated fin-shaped cavity. Khan et al.[17] used interesting Galerkin numerical scheme suggest the solution of a problem based on an unsteady flow of Eyring–Powell nano-material. A wavelet approach based theoretical investigation for the stagnation point flow of Williamson nanofluid has been directed by Hamid and co-researchers.[18] Usman et al.[19] used the modified wavelets scheme for the flow of nanofluid accounted by infinitely parallel plates. Khan et al.[20] studied the diffusive flow of nanofluid in porous cavity with combined features of heat and mass transportation. The triple diffusive flow of nanofluid with entropy generation assessment in horizontal plate has been directed by Khan et al.[21]

Following to the motivation applications of non-Newtonian nano-materials and entropy generation phenomenon, current research aims to explore the slip flow of Jeffrey nanofluid in presence of entropy generation and various thermal features. The novel features of current work are summarized as follows:

❖ To examine the heat transfer phenomenon in flow of Jeffrey nanofluid over a stretched configuration.
❖ The impact of activation energy and viscous dissipation effects has also been introduced as a novelty.
❖ The entropy generation phenomenon is addressed with thermodynamic approach.
❖ The partial slip features utilized to examine the flow pattern.
❖ The characteristics of thermophoresis and Brownian motion mechanism are addressed by employing Buongiorno model of nanofluid.
❖ he distinct flow characteristics of various parameters are discussed through graphs with relevant physical justification.

Modeling

Here, two dimensional, steady and incompressible slip flow of Jeffrey fluid is examined. Heat and mass transfer flow is discussed in presence of viscous dissipation, activation energy and Buongiorno model of nanofluid. The stretching sheet causes the flow of non-Newtonian fluid as shown in Figure 1. In cartesian coordinate plane, the velocity components u and v are utilized along the $x-$axis and normal direction, respectively. The activation energy relations are employed by following Arrhenius model. Entropy generation due to all these effects in the system is also discussed. Following equations are constituted for the formulated flow problem:

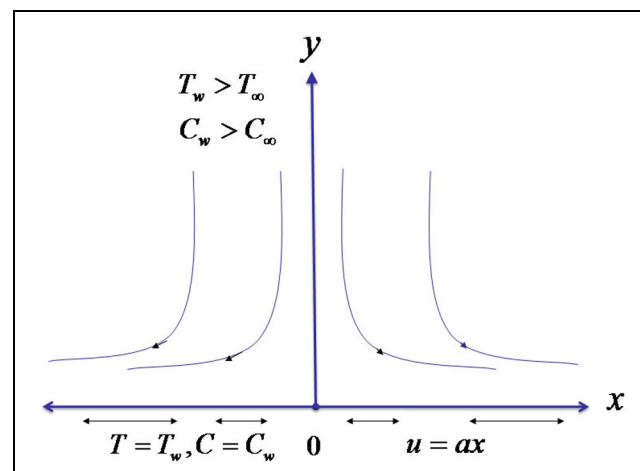$$\frac{\partial u}{\partial x} + \frac{\partial v}{\partial y} = 0, \tag{1}$$

Figure 1. Geometry of flow problem.

$$u\frac{\partial u}{\partial x} + v\frac{\partial u}{\partial y} = \frac{\nu}{1+\lambda_2}$$
$$\left[\frac{\partial^2 u}{\partial y^2} + \lambda_1\left(u\frac{\partial^3 u}{\partial x\partial y^2} + \frac{\partial u}{\partial y}\frac{\partial^2 u}{\partial x\partial y} - \frac{\partial u}{\partial x}\frac{\partial^2 u}{\partial y^2} + v\frac{\partial^3 u}{\partial y^3}\right)\right], \tag{2}$$

$$u\frac{\partial T}{\partial x} + v\frac{\partial T}{\partial y} = \frac{k_f}{(\rho c_p)_f}\frac{\partial^2 T}{\partial y^2} + \frac{\mu_f}{(\rho c_p)_f(1+\lambda_2)}$$
$$\left[\left(\frac{\partial u}{\partial y}\right)^2 + \lambda_1\left(v\frac{\partial u}{\partial y}\frac{\partial^2 u}{\partial y^2} + u\frac{\partial u}{\partial y}\frac{\partial^2 u}{\partial y\partial x}\right)\right] + \tag{3}$$
$$\frac{(\rho c_p)_s}{(\rho c_p)_f}\left[D_B\frac{\partial T}{\partial y}\frac{\partial C}{\partial y} + \frac{D_T}{T_\infty}\left(\frac{\partial T}{\partial y}\right)^2\right],$$

$$u\frac{\partial C}{\partial x} + v\frac{\partial C}{\partial y} = D_T\frac{\partial^2 C}{\partial y^2} - k_0^2(C - C_\infty)\left(\frac{T}{T_\infty}\right)^n Exp\left[\frac{-E_a}{\kappa T}\right], \tag{4}$$

with boundary conditions:[22,23]

$$u = ax + \frac{\beta_1}{1+\lambda_2}\left[\frac{\partial u}{\partial y} + \lambda_1\left(u\frac{\partial^2 u}{\partial y\partial x} + v\frac{\partial^2 u}{\partial y^2}\right)\right],$$
$$v = 0,\ T = T_w,\ C = C_w\ at\ y = 0, \tag{5}$$
$$u \to 0,\ T \to T_\infty,\ C \to C_\infty\ at\ y \to \infty.$$

In above expressions (x, y), μ_f, ρ_f, λ_1, λ_2, ν, k_f, c_p, β_1, a, (u, v), D_B, D_T, k_0^2, $(-1 < n < 1)$, T, T_∞, T_w, E_a, κ represent cartesian coordinates, dynamic viscosity, density, retardation time, ratio of relaxation to retardation times, kinematic viscosity, thermal conductivity, specific heat, velocity slip coefficient, stretching rate, velocity vectors, Brownian constant, thermophoretic coefficient, chemical reaction, fitted constant, temperature, ambient temperature, surface temperature, activation energy coefficient and Boltzmann constant.

Considering the dimensionless variables:

$$u = axf'(\xi),\ v = -\sqrt{a\nu}f,\ \theta(\xi) = \frac{T - T_\infty}{T_w - T_\infty},$$
$$\phi(\xi) = \frac{C - C_\infty}{C_w - C_\infty},\ \xi = \sqrt{\frac{a}{\nu}}y, \tag{6}$$

we arrive

$$\frac{1}{1+\lambda_2}\left(f''' - \lambda_3\left(ff^{(iv)} - f''^2\right)\right) + ff'' - f'^2 = 0, \tag{7}$$

$$\frac{1}{Pr}\theta'' + f\theta' + Nb\theta'\phi' + Nt\theta'^2 + \frac{Ec}{1+\lambda_2}$$
$$\left[f''^2 + \lambda_3\left(f'f''^2 - ff''f'''\right)\right] = 0 \tag{8}$$

$$\frac{1}{Sc}\varphi'' + f\phi' + \frac{Nt}{Nb}\theta'' - k_1\phi(1 + \delta\theta)^n Exp\left[\frac{-E_1}{1+\delta\theta}\right] = 0, \tag{9}$$

$$f'(0) = 1 + \frac{\beta_2}{1+\lambda_2}[f''(0) + \lambda_3 f'(0)f''(0)],$$
$$f(0) = 0,\ \theta(0) = 1, \tag{10}$$
$$\phi(0) = 1, f'(\infty) \to 0,\ \theta(\infty) \to 0,\ \phi(\infty) \to 0.$$

with λ_3 (retardation parameter), β_2 (slip parameter), Pr (Prandtl number), Nb (Brownian motion parameter), Ec (Eckert number), Nt (thermophoretic parameter), δ (temperature ratio parameter), Sc (Schmidt number), k_1 (chemical reaction parameter), and E_1 (activation energy parameter) which are defined as:

$$\lambda_3\left(= \lambda_1 a\right),\ Pr\left(= \frac{\nu_f}{\alpha_f}\right), Ec\left(= \frac{(ax)^2}{c_p(T_w - T_\infty)}\right), Nb\left(= \frac{(\rho c_p)_s D_B(C_w - C_\infty)}{(\rho c_p)_f \nu}\right), Nt\left(= \frac{(\rho c_p)_s D_T(T_w - T_\infty)}{(\rho c_p)_f \nu T_\infty}\right),$$
$$\beta_2\left(= \beta_1\sqrt{\frac{a}{\nu}}\right), Sc\left(= \frac{\nu_f}{D_B}\right),\ k_1\left(= \frac{k_0^2}{a}\right), \delta\left(= \frac{T_w - T_\infty}{T_\infty}\right),\ E_1\left(= \frac{E_a}{\kappa T_\infty}\right). \tag{11}$$

Mathematically, entropy generation in presence of above assumptions is addressed as:

$$S_G = \frac{\mu_f}{T_\infty}\frac{1}{1+\lambda_2}\left[\left(\frac{\partial u}{\partial y}\right)^2 + \lambda_1\left(v\frac{\partial u}{\partial y}\frac{\partial^2 u}{\partial y^2} + u\frac{\partial u}{\partial y}\frac{\partial^2 u}{\partial y\partial x}\right)\right]$$
$$+ \frac{R^*D}{T_\infty}\left(\frac{\partial T}{\partial y}\right)\left(\frac{\partial C}{\partial y}\right)$$
$$+ \frac{R^*D}{C_\infty}\left(\frac{\partial C}{\partial y}\right)^2 + \frac{k}{T_\infty^2}\left(\frac{\partial T}{\partial y}\right)^2, \tag{12}$$

dimensionless form is

$$N_G = \delta\theta'^2 + \frac{Ec}{1+\lambda_2}\left[f''^2 + \lambda_3\left(f'f''^2 - ff''f'''\right)\right]$$
$$+ L\theta'\phi' + L\frac{\delta_1}{\delta}\phi'^2. \tag{13}$$

The Bejan number is

$$Be = \frac{L\frac{\delta_1}{\delta}\phi'^2 + \delta\theta'^2 + L\theta'\phi'}{\delta\theta'^2 + \frac{Ec}{1+\lambda_2}[f''^2 + \lambda_3(f'f''^2 - ff''f''')] + L\theta'\phi' + L\frac{\delta_1}{\delta}\phi'^2}, \tag{14}$$

where $Br\left(= \frac{\mu_f(ax)^2}{k_f(\Delta T)}\right)$ reflects the Brinkman number, $L\left(= \frac{R^*D(C_w - C_\infty)}{k_f}\right)$ is diffusion parameter $\delta_1\left(= \frac{C_w - C_\infty}{C_\infty}\right)$ concentration difference constant and $N_G\left(= \frac{S_G T_\infty \nu}{k(\Delta T)a}\right)$ signify the entropy generation rate.
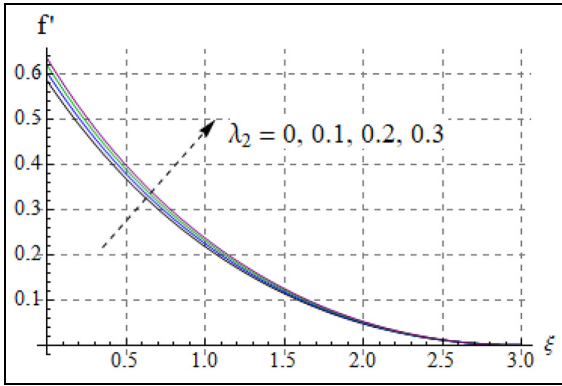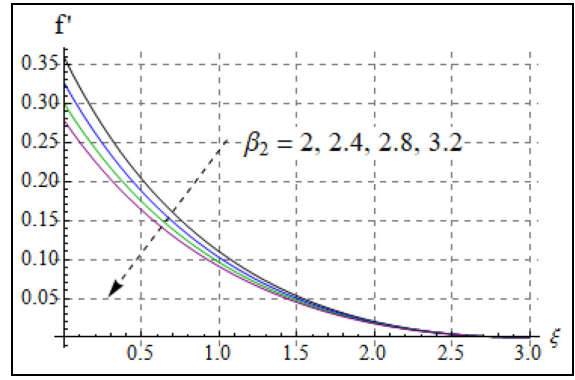
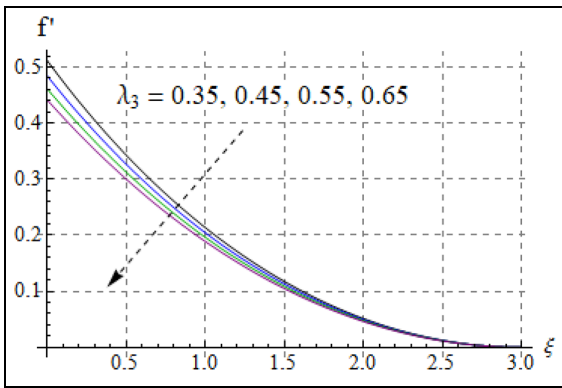**Figure 2.** $(f'(\xi))$ via λ_2.

Figure 4. $(f'(\xi))$ via β_2.

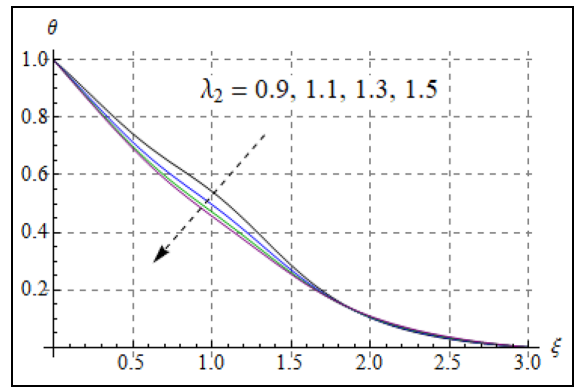**Figure 3.** $(f'(\xi))$ via λ_3.

Figure 5. $(\theta(\xi))$ via λ_2.

Expressions for physical quantities skin friction, Nusselt number and Sherwood number are presented below

$$\left.\begin{array}{l} C_{fx} = \dfrac{\tau_w}{\frac{\rho}{2}u_w^2(x)};\ \tau_w = \dfrac{\mu}{1+\lambda_2}\left[\dfrac{\partial u}{\partial y} + \lambda_1\left(u\dfrac{\partial^2 u}{\partial x \partial y} + u\dfrac{\partial^2 v}{\partial x^2} + v\dfrac{\partial^2 u}{\partial y^2}\right)\right]\bigg|_{y=0}, \\[3mm] Nu_x = \dfrac{xq_h}{k(T_f - T_\infty)};\ q_h = -k\dfrac{\partial T}{\partial y}, \\[3mm] Sh_x = \dfrac{xq_s}{D_B(C_f - C_\infty)};\ q_s = -D\dfrac{\partial C}{\partial y}, \end{array}\right\}$$

(15)

After implementation of transformation Eq. (15) takes the form

$$\left.\begin{array}{l} \dfrac{C_{fx}Re_x^{0.5}}{2} = \dfrac{1}{1+\lambda_2}[f''(0) + \lambda_3(f'(0)f''(0) - f(0)f'''(0))], \\[3mm] \dfrac{Nu}{\sqrt{Re_x}} = -\theta'(0), \\[3mm] \dfrac{Sh}{\sqrt{Re_x}} = -\phi'(0). \end{array}\right\}$$
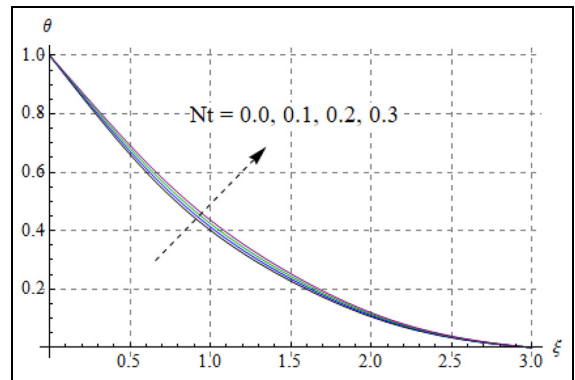
(16)

Figure 6. $(\theta(\xi))$ via Nt.

Discussion

Present section dedicated to analyze the behavior of velocity, concentration, temperature, entropy generation, Bejan number, Nusselt number, skin friction and Sherwood number versus different parameters (See Figures 2–16 and Tables 1–4).
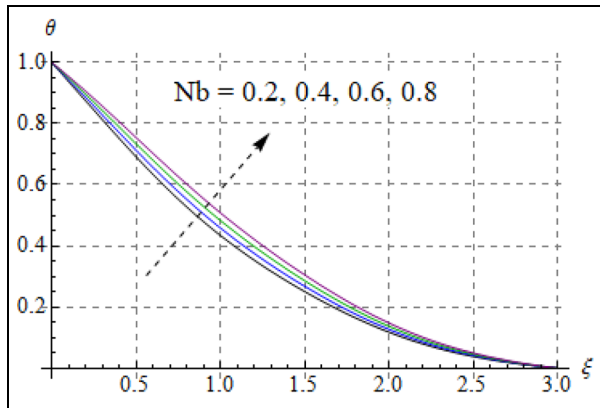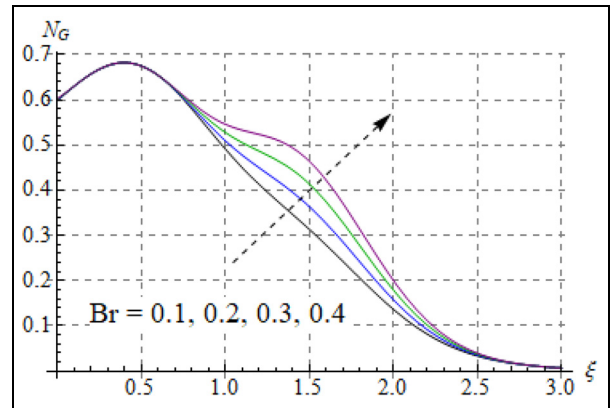
Figure 7. $(\theta(\xi))$ via *Nb*.
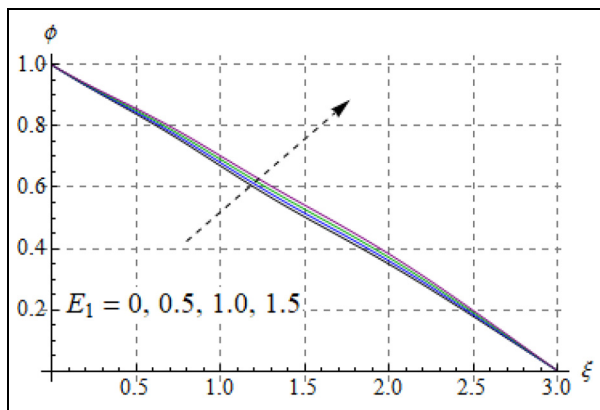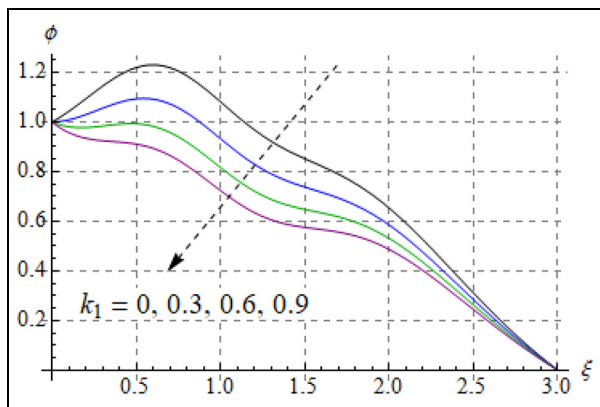

Figure 8. $(\phi(\xi))$ via E_1.

Figure 9. $(\phi(\xi))$ via k_1.

Impact of ratio of relaxation to retardation time parameter (λ_2), retardation time parameter (λ_3) and slip parameter (β_2) on velocity field is discussed in Figures 2 to 4. Figure 2 shows the impact of (λ_2) on $(f'(\xi))$. Increase in velocity is depicted for higher estimation of (λ_2). Physically, with increase in $(\lambda_2 = 0, 0.1, 0.2, 0.3)$ retardation time starts decline. It

Figure 10. $(N_G(\xi))$ via *Br*.

means that time taken by particles from perturbed to equilibrium system is decreasing so particles are moving faster. That is why $(f'(\xi))$ rises. Figure 3 is about the behavior of Deborah number $(\lambda_3 = 0.35, 0.45, 0.55, 0.65)$ along $(f'(\xi))$. As we know that retardation time is increasing function of Deborah number so particles are taken now more time it means velocity is decreasing. Impact of slip parameter via velocity field is seen in Figure 4. There is decrease in velocity for greater estimation of $(\beta_2 = 2, 2.4, 2.8, 3.2)$. Physically when slip between sheet and fluid particles adjacent to the sheet increases then stretching effect does not transfer fully to the fluid that is why velocity decays.

Figures 5 to 7 describe the behavior of (λ_2), thermophoretic parameter (Nt) and Brownian motion parameter (Nb) against temperature field. Figure 5 tells the impact of (λ_2) on temperature field. Temperature of the fluid is shown to be decreasing for rising $(\lambda_2 = 0.9, 1.1, 1.3, 1.5)$. Influence of thermophoretic parameter (Nt) on temperature is shown in Figure 6. With increase in Nt temperature difference enhances it means that particles travel from hotter region to colder region consequently temperature of the fluid increases $\theta(\xi)$. Figure 7 delineates the impact of (Nb) on temperature profile $\theta(\xi)$. Random motion of particles starts increases when we rise the values of (Nb) due to which $\theta(\xi)$ enhances.

Figures 8 and 9 exhibit the impact of activation energy parameter (E_1) and chemical reaction parameter (k_1) against concentration parameter $\varphi(\xi)$. Figure 8 reveals the effect of (E_1) on concentration profile. When activation energy enhances $Exp\left[\frac{-E_1}{1+\delta\theta}\right]$ Arrhenius function decays due to which less chemical reaction occur hence concentration profile reduces. Figure 9 explains the effect of (k_1) on $\varphi(\xi)$. Concentration profile reduces for higher (k_1).

Figures 10 to 15 are sketched to examine the influence of various parameters on entropy generation and Bejan number. Figures 10 and 11 reveal the impact of
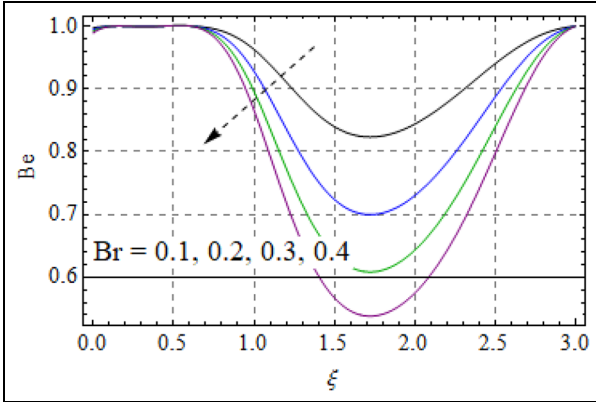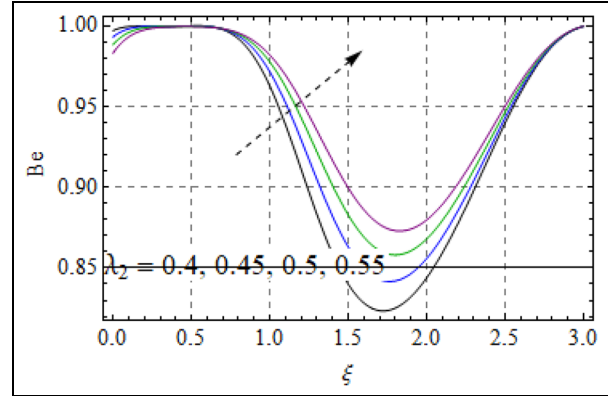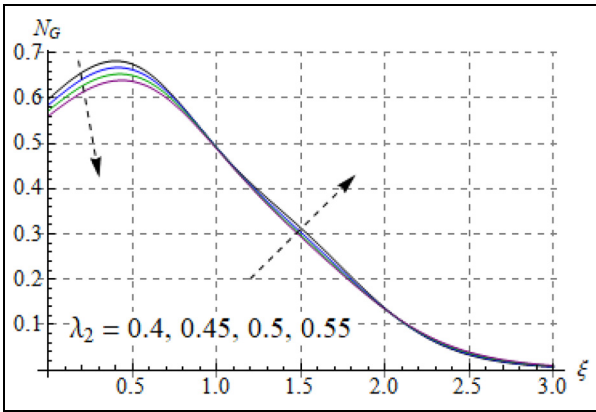
Figure 11. Be via Br.

Figure 13. Be via λ_2.

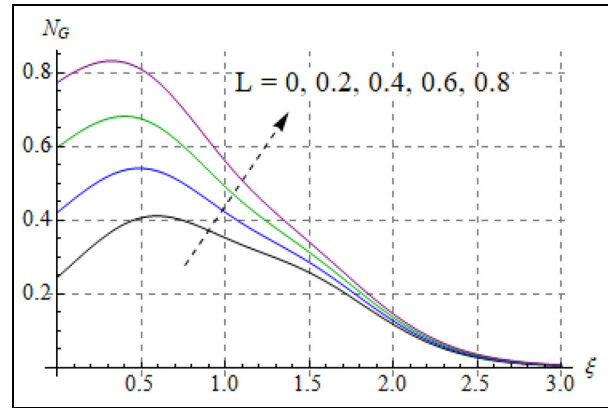**Figure 12.** $(N_G(\xi))$ via λ_2.

Figure 14. $(N_G(\xi))$ via L.

Brinkman number versus (N_G) and (Be). For increasing values of Br disturbance in the system also increases because Br attains direct relation with fluid viscosity. So for higher viscous dissipation irreversibility entropy also rises. There is decrease in Bejan number for increasing values of Brinkman number. It means viscous effects are prominent over mass and heat transfer irreversibility. Figures 12 and 13 are about the impact of (λ_2) via Bejan number and entropy generation. Entropy generation and Bejan show rising effect near the sheet for greater (λ_2) while show decreasing impact as we see away from the sheet. Figures 14 and 15 portray the influence of diffusion parameter (L) via entropy generation and Bejan number. There is increase in entropy generation and Bejan number for higher estimation (L). Mass transfer irreversibility have prominent effect as compared to viscous dissipation irreversibility due to increase in diffusion that is why Bejan number increases.

Figure 16 is drawn to show that average total residual error is decreasing with increasing order of approximation which shows the stability of our problem. We have found the optimal values of $\hbar_f$, $\hbar_\theta$ and
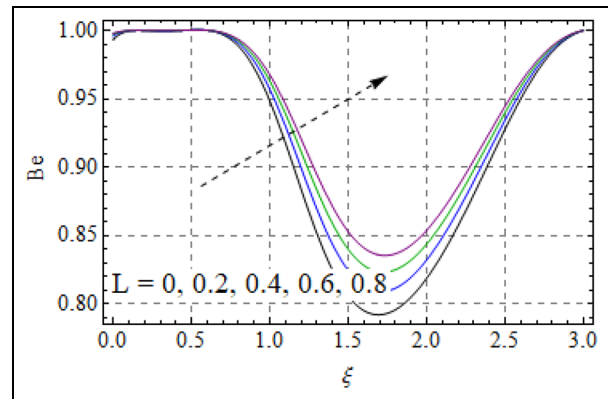
Figure 15. Be via L.

$\hbar_\varphi$ by using minimization concept using average squared residual errors as

$$\varepsilon_m^f = \frac{1}{k^\circ + 1} \sum_{j=0}^{k^\circ} \left[N_f \left(\sum_{i=0}^{m} f(\xi) \right)_{\xi = j\delta\xi} \right]^2, \quad (17)$$
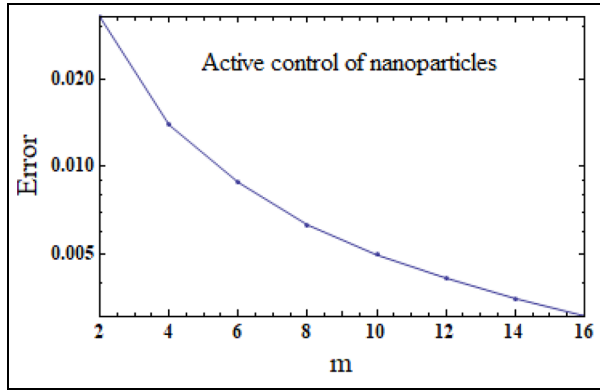
Figure 16. Total averaged squared residual error.

Table 1. Error analysis for velocity, temperature and concentration profile.

m	ε_m^f	ε_m^θ	ε_m^φ
2	0.000904599	0.0183986	0.0133041
4	0.0000757466	0.00667958	0.00713502
8	0.0000297458	0.00201959	0.00426175
10	0.0000153005	0.0013298	0.00363234
12	0.000025186	0.00093321	0.00318696
14	0.0000360966	0.000663046	0.00282848
16	0.0000180503	0.000496793	0.00255905

$$\varepsilon_m^\theta = \frac{1}{k^\circ + 1} \sum_{j=0}^{k^\circ} \left[\mathbf{N}_\theta \left(\sum_{i=0}^m \theta(\xi), \sum_{i=0}^m f(\xi), \sum_{i=0}^m \phi(\xi) \right)_{\xi = j\delta\xi} \right]^2,$$
(18)

$$\varepsilon_m^\varphi = \frac{1}{k^\circ + 1} \sum_{j=0}^{k^\circ} \left[\mathbf{N}_\phi \left(\sum_{i=0}^m \phi(\xi), \sum_{i=0}^m f(\xi), \sum_{i=0}^m \theta(\xi) \right)_{\xi = j\delta\xi} \right]^2,$$
(19)

Letting

$$\varepsilon_m^t = \varepsilon_m^f + \varepsilon_m^\theta + \varepsilon_m^\phi,$$
(20)

where ε_m^t is total error, $\delta\xi = 0.5$ and $k^\circ = 20$. Here we are using Mathematica package BVPh2.0 to minimize the average squared residual error. At 2nd order of approximations optimal values of auxiliary parameters are $h_f = -1.84975$, $h_\theta = 0.835461$, and $h_\varphi = -0.331413$ and $\varepsilon_m^t = 0.0326073$. Table 1 shows the residual errors for velocity, temperature and concentration profile separately by using optimal values at $m = 2$. Here we can see from Table 1 that squared residual error decreases with higher order of approximation.

Tables 2 to 4 describe the results of skin friction Nusselt number and Sherwood number against involved parameters. Here we have seen that drag force at surface reduces for higher values of λ_2, λ_3 and β_2

Table 2. Skin friction for variation of λ_2, λ_3 and β_2.

λ_2	λ_3	β_2	Skin friction
0.2	0.3	0.1	0.711096
0.3			0.102321
0.4			0.032422
0.5			0.000831
0.2	0.4		0.151763
	0.5		0.116727
	0.6		0.02023
	0.3	0.2	0.564604
		0.3	0.466897
		0.4	0.397519

Table 3. Nusselt number for variation of Nt, Nb and Ec.

Nt	Nb	Ec	Nusselt number
0.1	0.2	0.4	0.64055
0.2			0.609484
0.3			0.580321
0.1	0.3		0.615257
	0.4		0.590507
	0.2	0.5	0.605403
		0.6	0.570045

Table 4. Sherwood number for variation of Sc, Nt and E_1.

Sc	Nt	E_1	Sherwood number
0.1	0.1	0.4	0.448442
0.2			0.554274
0.3			0.651976
0.1	0.2		0.437395
	0.3		0.429055
	0.1	0.5	0.446793
		0.6	0.445126

(See Table 2). Nusselt number (heat transfer rate) is showing decreasing behavior for greater values of Nt, Nb and Ec. Sherwood number impact against Sc, Nt and activation energy parameter is shown in Table 4. It is observed that mass transfer rate declines for higher Nt and activation energy parameter while enhances for Schmidt number Sc.

Conclusions

The optimized flow of Jeffrey nanofluid in presence of partial slip confined by a stretched surface has been analyzed in this communication. The additional impact of viscous dissipation and activation energy are also addressed as a novelty. The numerical simulations are performed which is based on MATHEMAITCA

built-in ND scheme. The accuracy of solution is verified by performing error analysis. The main observations form present research work is summarized as:

> ➤ Theelocity profile enhances for ratio of relaxation to retardation time parameter while it decays for rising values of retardation time parameter.
> ➤ The presence of slip offers more resistance to fluid flow.
> ➤ An impvsed temperature is examined with thermophoretic and Brownian constants.
> ➤ The presence of activation is more efficient to improve the nanofluid concentration.
> ➤ The Bejan number and entropy generation parameter shows an increasing trend for diffusion
> ➤ An increasing entropy generation profile is observed with Brinkman number.

Declaration of conflicting interests

Funding

ORCID iDs

Faisal Shah https://orcid.org/0000-0003-0198-5959
M Ijaz Khan https://orcid.org/0000-0002-9041-3292

References

1. Ramesh K. Effects of viscous dissipation and Joule heating on the Couette and Poiseuille flows of a Jeffrey fluid with slip boundary conditions. *Propuls Power Res* 2018; 7: 329–341.
2. Kumar SG, Varma SVK, Raju SSK, et al. Three-dimensional conducting flow of radiative and chemically reactive Jeffrey fluid through porous medium over a stretching sheet with Soret and heat source/sink effects. *Results Eng*. Epub ahead of print 16 May 2020. DOI: 10.1016/j.rineng.2020.100139.
3. Ramesh GK, Kumara BCP, Gireesha BJ, et al. Casson fluid flow near the stagnation point over a stretching sheet with variable thickness and radiation. *J Appl Fluid Mech* 2016; 9: 1115–1122.
4. Xun S, Zhao J, Zheng L, et al. Flow and heat transfer of Ostwald-de Waele fluid over a variable thickness rotating disk with index decreasing. *Int J Heat Mass Trans* 2016; 103: 1214–1224.
5. Farooq M, Khan MI, Waqas M, et al. MHD stagnation point flow of viscoelastic nanofluid with non-linear radiation effects. *J Mol Liq* 2016; 221: 1097–1103.
6. Lin Y, Zheng L, Zhang X, et al. MHD pseudo-plastic nanofluid unsteady flow and heat transfer in a finite thin film over stretching surface with internal heat generation. *Int J Heat Mass Trans* 2015; 84: 903–911.
7. Hashim MK and Hamid A. Numerical investigation on time-dependent flow of Williamson nanofluid along with heat and mass transfer characteristics past a wedge geometry. *Int J Heat Mass Trans* 2018; 118: 480–491.
8. Hayat T, Qayyum S, Imtiaz M, et al. Impact of Cattaneo-Christov heat flux in Jeffrey fluid flow with homogeneous-heterogeneous reactions. *PLoS One* 2016; 11: e0148662.
9. Chaudhuri S and Das PK. Semi-analytical solution of the heat transfer including viscous dissipation in the steady flow of a Sisko fluid in cylindrical tubes. *J Heat Transfer* 2018; 140: 071701.
10. Hayat T, Qayyum S, Imtiaz M, et al. Radiative Falkner-Skan flow of Walter-B fluid with prescribed surface heat flux. *J Theor Appl Mech* 2017; 55: 117–127.
11. Choi SUS and Eastman JA. Enhancing thermal conductivity of fluids with nanoparticles. In: *Proceedings of the ASME international mechanical engineering congress and exposition*, San Francisco, CA, USA, 12–17 November 1995. ASME.
12. Hayat T, Khan MI, Qayyum S, et al. Entropy generation in flow with silver and copper nanoparticles. *Colloid Surf A* 2018; 539: 335–346.
13. Krishnamurthy MR, Prasannakumara BC, Gorla RSR, et al. Non-linear thermal radiation and slip effect on boundary layer flow and heat transfer of suspended nanoparticles over a stretching sheet embedded in porous medium with convective boundary conditions. *J Nanofluids* 2016; 5: 522–530.
14. Kumar KG, Gireesha BJ, Kumara BC, et al. Impact of chemical reaction on marangoni boundary layer flow of a Casson nano liquid in the presence of uniform heat source sink. *Diffus Found* 2017; 11: 22–32.
15. Roja A, Gireesha BJ and Prasannakumara BC. MHD micropolar nanofluid flow through an inclined channel with entropy generation subjected to radiative heat flux, viscous dissipation and multiple slip effects. *Multidiscip Model Mater Struct* 2020; 16: 1475–1496.
16. Hamid M, Khan ZH, Khan WA, et al. Natural convection of water-based carbon nanotubes in partially heated rectangular fin-shaped cavity with inner cylindrical obstacle. *Phys Fluids* 2019; 31: 103607.
17. Khan ZH, Usman M, Zubair T, et al. Brownian motion and thermophoresis effects on unsteady stagnation point flow of Eyring–Powell nanofluid: a Galerkin approach. *Commun Theor Phys* 2020; 72: 125005.
18. Hamid M, Usman M, Haq RU, et al. Wavelet analysis of stagnation point flow of non-Newtonian nanofluid. *Appl Math Mech* 2019; 40: 1211–1226.
19. Usman M, Zubair T, Hamid M, et al. Novel modification in Wavelets method to analyze unsteady flow of nanofluid between two infinitely parallel plates. *Chin J Phys* 2020; 66: 222–236.
20. Khan ZH, Khan WA and Sheremet MA. Enhancement of heat and mass transfer rates through various porous cavities for triple convective-diffusive free convection. *Energy* 2020; 201: 117702.

21. Khan ZH, Khan WA, Tang J, et al. Entropy generation analysis of triple diffusive flow past a horizontal plate in porous medium. *Chem Eng Sci* 2020; 228: 115980.

22. Das K, Acharya N and Kundu PK. Radiative flow of MHD Jeffrey fluid past a stretching sheet with surface slip and melting heat transfer. *Alexandria Eng J* 2015; 54: 815–821.

23. Turkyilmazoglu M. Magnetic field and slip effects on the flow and heat transfer of stagnation point Jeffrey fluid over deformable surfaces. *Z Naturforsch A* 2016; 71: 549–556.

Appendix

Notation

(x, y)	
ρ_f	density
λ_2	ratio of relaxation to retardation times
k_f	thermal conductivity
β_1	velocity slip coefficient
(u, v)	velocity vectors
D_T	thermophoretic diffusion coefficient
T	temperature
T_w	surface temperature
κ	Boltzmann constant
β_2	slip parameter
Nb	Brownian motion parameter
Ec	Eckert number
k_1	chemical reaction parameter
E_1	activation energy parameter
N_G	entropy generation
L	diffusion parameter
N_G	entropy generation rate
μ_f	dynamic viscosity
λ_1	retardation time
ν	kinematic viscosity
c_p	specific heat
a	stretching rate
D_B	Brownian diffusion coefficient
k_0^2	chemical reaction rate
T_∞	ambient temperature
E_a	activation energy coefficient
λ_3	retardation parameter
Pr	Prandtl number
Nt	Thermophoretic parameter
Sc	Schmidt number
δ	temperature ratio parameter
Be	Bejan number
Br	Brinkman number
δ_1	concentration difference parameter